Role of miR-29b on the regulation of the extracellular matrix in human trabecular meshwork cells under chronic oxidative stress

Coralia Luna, Guorong Li, Jianmimg Qiu, David L. Epstein, Pedro Gonzalez

Department of Ophthalmology, Duke University, Durham, NC

Purpose: To investigate the role of miR-29b on the changes in expression of genes involved in the synthesis and deposition of extracellular matrix (ECM) induced by chronic oxidative stress in human trabecular meshwork cells (HTM).

Methods: Changes in gene expression induced by miR-29b in HTM cells were evaluated by gene array analysis using Affymetrix U133A2 arrays and confirmed by quantitative–PCR. Pathway analysis was conducted using Metacore. Targeting of miR-29b to the 3'-untranslated region of three novel putative targets was evaluated using the Psicheck luciferase system. Chronic oxidative stress was induced by incubation at 40% oxygen for 4–5 days, using cultures incubated at 5% oxygen as controls. Changes in expression in microRNA or gene expression were analyzed by Q-PCR. Cell viability was measured by lactate dehydrogenase release.

Results: Transfection of HTM cells with miR-29b mimic resulted in downregulation of multiple ECM components, including collagens (*COL1A1, COL1A2, COL4A1, COL5A1, COL5A2, COL3A1*) *LAMC1,* and *FBN* as well as several genes involved in ECM deposition and remodeling, such as *SPARC*/osteonectin. Three additional genes, *BMP1, ADAM12*, and *NKIRAS2*, were identified as direct targets of miR-29b. Chronic oxidative stress induced a significant downregulation of miR-29b in two HTM cell lines that was associated with increased expression of several ECM genes known to be regulated by miR-29b. The increase in expression of these genes was inhibited by transfection with miR-29b mimic. MiR-29b increased cell viability under both chronic oxidative stress and physiologic oxygen concentrations.

Conclusions: MiR-29b negatively regulates the expression of multiple genes involved in the synthesis and deposition of ECM in trabecular meshwork (TM) cells. Downregulation of miR-29b might contribute to increased expression of several ECM genes under chronic oxidative stress conditions. The balance between the activation of ECM production induced by oxidative stress and the protective effects of miR-29b could be a relevant factor in understanding how oxidative damage may lead to increased deposition of ECM in the TM and contribute to the elevation of intra-ocular pressure in glaucoma.

Chronic oxidative stress has been implicated in both the initiation and progression of pathophysiological phenomena in the trabecular meshwork (TM) in glaucoma [1-3]. Primary open-angle glaucoma (POAG) has been shown to be associated with a significant increase in the accumulation of the primary and secondary end products of lipid peroxidation in lipid extracts from TM, aqueous humor, and Schlemm's canal (SC) [3,4]. Similarly, significantly higher levels of the product of DNA oxidation 8-oxo-2,7-dihydro-20-deoxyguanosine have been observed in the TM of glaucoma patients compared with age-matched and sex-matched controls, and the levels of DNA damage were correlated significantly with elevation of intra-ocular pressure and visual field defects [1,2,5,6]. Furthermore, reactive oxygen species-mediated damage to the TM has been shown to induce alterations that result in increased aqueous humor outflow resistance [1,7].

Oxidative damage can lead to outflow tissue dysfunction through apoptotic cell loss [8] by inducing certain phenotypic alterations, including those associated with stress-induced senescence. One such phenotypic alteration that has been proposed to explain how oxidative damage might contribute to the malfunction of the TM is the induced upregulation of extracellular matrix (ECM) genes [9]. Such upregulation of ECM-related genes could potentially contribute to the accumulation of ECM components in the sheath-derived plaques (SD-plaques) that have been shown to increase in the TM with aging and in POAG [10]. However, the specific molecular mechanisms involved in the alterations in ECM induced by oxidative stress in TM cells are not completely understood.

MicroRNAs (miRNAs) are an abundant class of noncoding small (~22 nucleotides) RNAs that modulate gene expression at the post-transcriptional level and participate in the regulation of many cellular functions [11-13]. Specifically, miR-29b has been demonstrated to regulate multiple genes coding for ECM proteins, including multiple collagens, fibrillins, and elastin. MiR-29 is a positive regulator of osteoblast differentiation and controls the expression of collagens in differentiated osteoblasts [14]. This miRNA has also been found to be downregulated in various cancers [15-18] and targets extracellular matrix collagens in lung and nasopharyngeal cancer cells [18]. MiR-29b is also downregulated in myocardial infarct, and its downregulation

Correspondence to: Pedro Gonzalez, Department of Ophthalmology, Duke University, Durham, NC, 27710; Phone: (919) 681-5995; FAX: (919) 684-8983; email: gonza012@mc.duke.edu

TABLE 1. PRIMERS USED FOR AMPLIFICATION OF THE 3' UNTRANSLATED REGIONS OF *BMP1*, *ADAM12*, AND *NKIRAS2*.

Gene symbol	Forward 5'-3'	Reverse 5'-3'
BMP1	GGCTCGAGGGCCTGCCAGGCCTCCCG	GGGCGGCCGCGCAAGAGAAAGGAGCAGGAC
ADAM12	GGCTCGAGGTGAAGACAGAAGTTTGCAC	GGGCGGCCGCTCATATCCTCTTATAATTGG
NKIRAS2	GGGCTCGAGGCTGCCGTTCCTCTTTCACG	GGGGCGGCCGCGTGTCCAACCAATGCATCAA

TABLE 2. PRIMERS USED FOR Q-PCR AMPLIFICATION.

Gene symbol	FORWARD 5'-3'	REVERSE 5'-3'
STC1	TCAGAGACAGCCTGATGGAG	CCTCACCTCGGAGGTTCCTG
STC2	TCTGCACCTCGGCCATCCAG	TCAGAATACTCAGACTGTTC
COL4A1	CCTGGCTTGAAAAACAGCTC	AGGCCTAGTGGTCCGAATCT
CRABP2	GTGATGCTGAGGAAGATTGC	CCACAGTCTGCTCCTCAAAC
TIMP3	TGCAGCTGGTACCGAGGATG	CAGGCACTAATTTCATTGTC
LOXL2	TACCTGGAGGACCGGCCCATG	AGGTCATAGTGGGTGAACAC
COL1A1	AGCCAGCAGATCGAGAACAT	TCTTGTCCTTGGGGGTTCTTG
COL1A2	TGCAAGAACAGCATTGCATAC	GGCAGGCGAGATGGCTTATTTGTT
COL3A1	CCATGAATGGTGGTTTTCAG	GTGTTTAGTGCAACCATC
COL5A1	GGCTGTGCTACCAAGAAAGG	GAGGTCACGAGGTTGCTCT
COL5A2	TGATCCTGAGACTCTTGAAG	GGTGGTCATTGTCATTGGTC
LAMC1-1	AATGAAGCCAAGAAGCAGGA	ATGGACAGCAGCAGAGGAGT
SPARC	CCGGGACTTCGAGAAGAACT	CTCATCCAGGGCAATGTACT
FBN1	CTGCAAGAGGATGGAAGGAG	GGTAAATCCGGGAGGACATT
BMP1	GTGTGGCCCGATGGGGTCAT	CCCGCAAGGTCGATAGGTGAA
ADAM12	ATGTGGAAAAATCCAGTGTC	GCAAGCACAAGCCCTGGGTC
NKIRAS2	CAGGAGCAGCGGCGTGTAGA	GCCATCCAAGGAGCCGCTGC
ACTB	CCTCGCCTTTGCCGATCCG	GCCGGAGCCGTTGTCGACG

has been shown to contribute to fibrosis in the heart [19]. Thus, miR-29 would be predicted to contribute to the regulation of ECM dynamics in the TM. However, the roles of this miRNA in the TM and the potential involvement on the alterations in ECM synthesis induced by oxidative stress in TM cells have not been investigated.

To gain more insight into the potential role of miR-29b in the TM, we investigated the effects of chronic oxidative stress on the expression of miR-29b, analyzed the changes in gene expression mediated by miR-29b, and evaluated whether alterations in miR-29b expression might alter the effects induced by chronic oxidative stress in human TM (HTM) cells.

METHODS

Cell cultures and oxidative stress conditions: HTM cell cultures were generated from cadaver eyes, with no history of eye disease, within 48 h post mortem, as previously reported [20]. All procedures involving human tissue were conducted in accordance with the tenets of the Declaration of Helsinski. Cell cultures were maintained at 37 °C in 5% CO_2 in media (low glucose Dulbecco's Modified Eagle Medium with L-glutamine, 110 mg/ml sodium pyruvate, 10% fetal bovine serum, 100 µM nonessential amino acids, 100 units/ml penicillin,100 µg/ml streptomycin sulfate, and 0.25 µg/ml amphotericin B). All the reagents were obtained from Invitrogen Corporation (Carlsbad, CA). Oxidative stress was induced by incubation at 40% oxygen 5% CO_2 for 4–5 days. Cells incubated at 40% oxygen were compared to cells incubated at an oxygen concentration close to the physiological concentration reported in the aqueous humor (oxygen partial pressure PO_2 5%) [21].

Transfections: HTM cells were plated 24 h before transfection with hsa-miR-29b mimic or control mimic (scramble; 20-40pmolar [Dharmacon, Chicago, IL] with Lipofectamine 2000 [Invitrogen] or amaxa nucleofactor kit [Lonza, Basel, Switzerland]) following the manufacturer's instructions. Briefly, for nucleofection, cells were transfected at density of 4×10^6 using an endothelial nucleofactor Kit and the program T23 in the Nucleofector, following the basic protocol for primary mammalian endothelial cells and 20 picomolar of miRNAs (Amaxa, scientific-support.US@amaxa.com). For lipofectamine transfections, cells were seeded at $2-3 \times 10^5$ cells in 12 well plates or $5-6 \times 10^5$ cells in 6 well plates using 40 picomolar miRNAs and 1 or 2 µl of lipofectamine (for 12 and 6 well plates, respectively) and OPTI-MEM I (Invitrogen). Cotransfections of 293A cells with luciferase 3'untranslated region (UTR) constructs (0.3 µg), miR-29b mimic, or control mimic (20 pmolar) were accomplished using Effectene (Qiagen, Valencia, CA).

Gene microarray analysis: Gene array analysis was conducted in three independent sets of transfections with

either miR-29b mimic or mimic control of the same HTM cell line. Total RNA was extracted three days post transfection using RNeasy kit (Qiagen), amplified (one round amplification) using one cycle target labeling and control reagents (Affymetrix, Santa Clara, CA), and hybridized to human genome U133A2 arrays (Affymetrix) at the Duke University Microarray facility. Raw data were normalized and analyzed using GeneSpring 7.3 (Silicon Genetics, Santa Clara, CA). Genes were filtered to their intensities in the control channel. Pre-mixed polyadenylated prokaryotic sequences from the One cycle target labeling and control reagents kit (Affymetrix) were spiked directly into the samples before target labeling and used as controls. Raw data values below 100 were considered as unreliable. Intensity-dependent normalization was performed per spot and per chip (LOWESS normalization). ANOVA test was performed (p-values ≤0.05 were considered significant) for genes differentially expressed, using the Benjamin and Hochberg False Discovery Rate correction test. The list of genes were compared to three databases that predict targets for miRNAs: Microcosm, TargetScan, and PicTar-Vert. To study the potential biological significance of the changes observed in the arrays, we performed network analysis of differentially expressed genes, using Metacore pathway analysis (GeneGo, St. Joseph, MI).

Analysis of miR-29b interaction with 3' untranslated regions: The entire 3'UTRs from bone morphogenic protein 1 (*BMP1*), ADAM metallopeptidase domain 12 *(ADAM12)*, and *NFKB* inhibitor-interacting Ras-like protein 2 (*NKIRAS2*) were amplified using primers in Table 1, with carried XhoI and NotI restriction sites in the forward or the reverse position. PCR amplifications from 3'UTRs and the complementary sequences were confirmed by sequencing and cloned into XhoI and NotI sites downstream of Renilla luciferase in the psiCheck2 vector (Promega, Madison, WI). For analysis of luciferase activity, 293A cells were seeded in 12-well culture dishes 24 h before transfection and transfected with psicheck 3'UTR, or the complementary sequence from BMP1, ADAM12, or NKIRAS2 (300 ng), and miRNAs for 29b mimic or control mimic. Luciferase was measured using the Dual Luciferase Kit (Promega, Madison, WI) following manufacturer's instructions and read in a TD-20/20 luminometer (Turner Designs, Sunnyvale, CA). In this assay, the activities of *Photinus pyralis* and *Renilla reniformis* luciferases are measured sequentially from a single sample. The firefly reporter is measured first by adding Luciferase Assay Reagent II to generate a luminescent signal. After quantifying the firefly luminescence, this reaction is quenched, and the *Renilla* luciferase reaction is simultaneously initiated by adding Stop & Glo® Reagent to the same tube.

RNA isolation and Quantitative PCR: Total RNA was isolated using an RNeasy kit (Qiagen Inc.) or Trizol (Invitrogen)

extraction, according to the manufacturer's instructions. RNA yields were measured using RiboGreen fluorescent dye (Invitrogen). First-strand cDNA was synthesized from total RNA (1 µg) by reverse transcription using oligodT and Superscript II reverse transcriptase (Invitrogen), according to the manufacturer's instructions. Quantitative (Q)-PCR reactions were performed in a 20-µl mixture containing 1 µl of the cDNA preparation, 1X iQ SYBR Green Supermix (Bio-Rad, Hercules, CA), using the following PCR parameters: 95 °C for 5 min followed by 50 cycles of 95 °C for 15 s, 65 °C for 15 s and 72 °C for 15 s. β-Actin was used as an internal standard of mRNA expression. The absence of nonspecific products was confirmed by both the analysis of the melt curves and by electrophoresis in 3% Super AcrylAgarose gels (DNA technology, Risskov, Denmark). The primers used for Q-PCR amplification are shown in Table 2. MicroRNAS were extracted using RT^2 qPCR-Grade miRNA isolation kit (SABiosciences, Frederick, MD) from total RNA extracted with Trizol. miRNAs cDNA (25 ng) were amplified using TaqMan microRNA reverse transcription Kit (Applied Biosystems, Foster City, CA) and specific primers for miR-29b and U6B (Applied Biosystems), as a standard. Q-PCR products were amplified using TaqMan® Universal PCR Master Mix (Applied Biosystems), following manufacturer's instructions. Briefly, TaqMan quantification is a two step process, in the reverse transcription step cDNA was reverse transcribed from RNA enriched with miRNAs using miR29b and U6B specific primers. PCR products were amplified from these cDNAs using 29b and U6b probes and the recommended PCR parameters: 95 °C for 10 min followed by 40 cycles of 95 °C for 15 s and 60 °C for 1 min. During PCR, the probe anneals specifically to a complementary sequence between the forward and reverse primer sites, when the probe is intact the proximity of the reporter dye to the quencher dye results in suppression of reporter fluorescence. The DNA polymerase cleaves only probes that are hybridized to the target, the cleavage separate the reporter from the quencher and this separation results in increased fluorescence by the reporter. The fluorescence threshold value (C_t) was calculated using the iCycle system software (Bio-Rad). The results were expressed as mean value± SE (standard error) in three independent experiments.

Cell viability assay: To evaluate changes in cell viability induced by miR-29b, cells were transfected with control mimic or miR-29b mimic. Cell viability was assayed after 5 days at 40% and 5% oxygen, by measuring the lactate dehydrogenase released to the culture media as a result of plasma membrane damage using the Cito Tox 96® Non-Radioactive Cytotoxicity assay (Promega) following the manufacturers instructions. Briefly, LDH was measured in culture supernatants and in cell lysates from each well, in a 30-min coupled enzymatic reaction, which results in the conversion of a tetrazolium salt (INT) into a red formazan product. The amount of color formed is proportional to the

TABLE 3. GENES UP-OR DOWN-REGULATED AFTER TRANSFECTION WITH HSA-MIR-29B IN HTM CELLS.

Genebank	Symbol	p value	Fold	Microcosm	Targetscan	Pictar
Selected genes up or down regulated by 2 fold or greater						
Down-regulated						
AF130082	*COL3A1*	0.0062	-4.310	*	*	*
AI983428	*COL5A1*	0.0065	-3.876			
N30339	*COL5A1*	0.0036	-3.597			
NM_000090	*COL3A1*	0.0068	-3.571	*	*	*
BC000658	*STC2*	0.0284	-3.356			
K01228	*COL1A1*	0.0154	-3.3		*	*
Y15916	*COL1A1*	0.0036	-3.268		*	*
AI300520	*STC1*	0.0177	-3.236			
AL575735	*COL5A2*	0.0036	-3.096		*	*
AI743621	*COL1A1*	0.0188	-3.086		*	*
W46291	*ADAM12*	0.0121	-3.077		*	
BE251211	*LOXL2*	0.0177	-3.03			
U05598	*AKR1C2*	0.0008	-2.959			
M33376	*AKR1C2*	0.0068	-2.915			
AW188198	*TNFAIP6*	0.0447	-2.817			
U46768	*STC1*	0.0275	-2.817			
AU144167	*COL3A1*	0.0068	-2.786	*	*	*
AL575735	*COL5A2*	0.0093	-2.695		*	*
AF117949	*LOXL2*	0.0163	-2.475			
NM_024089	*KDELC1*	0.0395	-2.463	*	*	*
NM_006186	*NR4A2*	0.0144	-2.445			
NM_007115	*TNFAIP6*	0.0144	-2.398			
NM_001353	*AKR1C1*	0.0079	-2.398			
NM_003155	*STC1*	0.0062	-2.375			
BE962749	*PPIC*	0.0036	-2.347	*	*	*
NM_003474	*ADAM12*	0.0342	-2.32		*	
AF118094	*TAF11*	0.0163	-2.232	*		
AL050136	*TMF1*	0.0072	-2.222			
S68290	*AKR1C1*	0.0065	-2.222			
AA530892	*DUSP1*	0.0236	-2.155			
AI922605	*COL4A1*	0.0157	-2.155	*	*	*
NM_004353	*SERPINH1*	0.0068	-2.146			
BC001131	*HIST1H2BG*	0.0263	-2.137			
NM_005689	*ABCB6*	0.0121	-2.123	*	*	*
NM_000943	*PPIC*	0.0275	-2.114	*	*	*
AL567376	*LYPD1*	0.0132	-2.058			
NM_000089	*COL1A2*	0.0181	-2.045	*	*	*
NM_006455	*SC65*	0.043	-2.004			
BC000055	*FSTL1*	0.0067	-2		*	*
Up-regulated						
NM_022817	*PER2*	0.0144	2.01			
NM_021245	*MYOZ1*	0.0144	2.354			
NM_006895	*HNMT*	0.0068	2.442			
NM_001878	*CRABP2*	0.0163	2.607			
Selected genes up or down regulated between 1.5 and 1.9 fold						
Down-regulated						
NM_004995	*MMP14*	0.0154	-1.953			
Z48481	*MMP14*	0.0275	-1.88			
NM_002293	*LAMC1*	0.0143	-1.689	*	*	*
BE222709	*MFAP3*	0.0063	-1.543	*	*	*
AL575922	*SPARC*	0.0062	-1.529		*	*
NM_000138	*FBN1*	0.0128	-1.529	*	*	*
Up-regulated						
NM_002575	*SERPINB2*	0.05	1.9			
NM_000362	*TIMP3*	0.0461	1.83			
NM_002160	*TNC*	0.0157	1.74			
NM_021111	*RECK*	0.0068	1.503			

This table shows genes that significantly change expression after transfection with miR-29b compared to controls by gene array analysis. The asterisks indicates the miRNA databases that predicts these genes as putative targets for miR29b.

TABLE 4. VALIDATION OF GENE EXPRESSION CHANGES AFTER TRANSFECTION WITH HSA-MIR29B.

Gene	Arrays		HTM -1		HTM-2		HTM-3	
symbol	Fold	p-value	Fold	p-value	Fold	p-value	Fold	p-value
COL1A2	-2.0450	0.0181	-1.5874	0.0086	-2.2974	0.0006	-2.1189	0.0104
COL5A2	-3.0960	0.0036	-2.7007	0.0013	-2.0946	0.0486	-1.9543	0.0410
COL5A1	-3.8760	0.0065	-1.8234	0.0095	-2.6390	0.0138	-2.4340	0.0017
COL3A1	-4.3100	0.0062	-3.0314	0.0167	-2.9622	0.0002	-2.1685	0.0088
COL1A1	-3.3003	0.0154	-1.7818	0.0019	-2.8945	0.0000	-2.0467	0.0416
COL4A1	-2.1552	0.0157	-2.5247	0.0078	-2.3217	0.0091	-1.4473	0.0042
STC1	-3.2362	0.0177	-1.4641	0.0132	1.0353	0.3437	-1.6818	0.0349
LOXL2	-2.4752	0.0163	-1.8234	0.0718	-1.7818	0.0044	-2.1936	0.0493
STC2	-3.3557	0.0284	-2.2191	0.0221	-1.4811	0.0029	-1.8234	0.0243
FBN1	-1.5291	0.0128	-1.6434	0.0015	-2.1435	0.0053	-1.6434	0.0500
LAMC1	-1.6892	0.0143	-1.7211	0.0184	-2.2449	0.0072	-1.9770	0.0136
SPARC	-1.5291	0.0062	-1.4641	0.0464	-2.5787	0.0066	-1.4983	0.0219
CRABP2	2.6070	0.0163	1.8446	0.0222	2.8284	0.0109	2.0467	0.0251
TIMP3	1.8300	0.0461	2.7638	0.0258	-1.3044	0.3918	1.9000	0.0311

Fold changes refers to the ratio of the expression values of the cells transfected with miR-29b over the cells transfected with scramble. P-values for the Q-PCR refer to the t-test between normalized C_T values in cells transfected with miR-29b versus cells transfected with scramble.
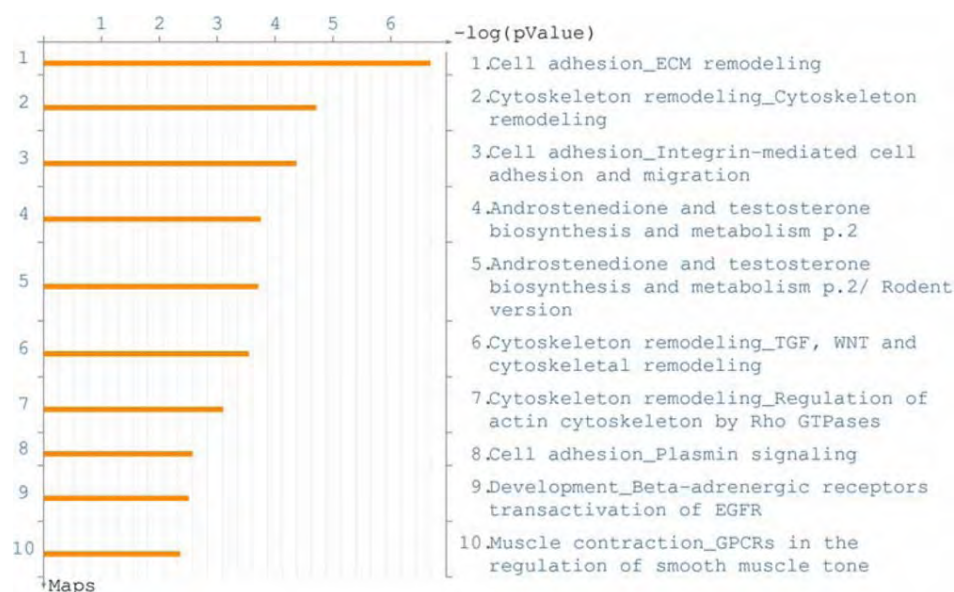

Figure 1. Pathway analysis of changes in gene expression induced by miR-29b. Genes showing changes in expression higher than 1.5 fold (p<0.05) after transfection with miR-29b mimic using Affymetrix U133A2 arrays were analyzed with Metacore pathway analysis. The canonical pathway maps used in this analysis represent a set of 650 signaling and metabolic maps generated from the GeneGo database (GeneGo, St. Joseph, MI). The figure shows the 10 canonical pathways most significantly affected by transfection with miR-29b mimic compared to controls. In the figure, ECM represents extracellular matrix; TGF represents transforming growth factor; EGFR represents epidermal growth factor; and GPCRs represents G protein-coupled receptors.

number of lysed cells. LDH in the supernatant was corrected for the total LDH (Supernatant/Supernatant + cell lysis). For each sample the quantification was performed in duplicate. The results were expressed as mean value±SE in three independent experiments.

RESULTS

Changes in gene expression induced by miR-29b in human trabecular meshwork cells: Differences in gene expression induced by miR-29b were evaluated by gene array analysis using Affymetrix U133A2 chips. HTM cells were transfected with miR-29b mimic and gene expression was compared to

that in cell cultures transfected with a control mimic. One hundred sixteen genes represented by 181 probes were significantly (p≤0.05) upregulated or downregulated more than 1.5-fold. Thirty-one percent of these transcripts were predicted in at least one of the three miRNA databases as putative targets for miR-29b. MiR-29b downregulated several ECM structural proteins, as collagens (*COL5A2, COL5A1, COL4A1, COL3A1, COL1A1*, and *COL1A2*) laminin C, fibrillin 1, and microfibrillar-associated protein 3; and extracellular matrix regulators, such as *MMP14, LOXL2, SERPINH1, SPARC, TNFAIP6*, and *ADAM 12*. Other matrix

regulators, such as plasminogen activator inhibitor 2, *RECK,* and *TIMP3,* showed upregulation. Table 3 shows transcripts upregulated or downregulated by more than twofold and some selected genes related to ECM that were significantly downregulated or upregulated between 1.5- and 1.9-fold.

To validate Affymetrix microarray data, changes in expression of 14 genes were analyzed by Q-PCR in three independent HTM cell lines different from the one used for array hybridization (Table 4).

Functional network analysis of gene expression changes induced by miR-29b: In order to identify the pathways and regulatory elements more likely associated with the changes in gene expression induced by miR-29b, genes significantly (p<0.5) upregulated or downregulated by 1.5-fold in the array analysis were further analyzed using MetaCore algorithms. The three canonical pathways most significantly affected by miR-29b are represented in Figure 1 and include cell adhesion–ECM remodeling (p=1.5 E-107); cytoskeleton remodeling (p=2 E-105), and cell adhesion–integrin-mediated cell adhesion and migration (p=4 E-105; Figure 1). Analysis of transcription factor regulation identified SP1 as the transcription factor most significantly (p=4.82 E-106) involved in the regulation of genes affected by miR-29b with 46 nodes (Figure 2).

Targeting of the 3' untranslated regions of BMP1, ADAM12, and NKIRAS2 mRNA by miR-29b: Computational predictions indicate that miR-29b shares complementarity with sequences in the 3'UTR of three genes found to be downregulated by miR-29b according to the gene array analysis: *BMP1, ADAM12,* and *NKIRAS2* (Figure 3A). We investigated whether miR-29b could interact with the 3'UTRs of these genes by using the psiCheck2 luciferase assay system. MiR-29b mimic significantly reduced luciferase expression in cells cotransfected with the 3'UTR of *BMP1, ADAM12,* or *NKIRAS2* compared to mimic control (scramble). The decrease in luciferase activity was completely or significantly prevented when the 3'UTR complementary sequences were used (Figure 3B). Downregulation of these gene transcripts by miR-29b was confirmed by Q-PCR in three HTM cells lines (Figure 3C).

Effects of chronic oxidative stress on the expression of miR-29b.: Changes in expression of miR-29b induced by chronic oxidative stress were analyzed by Q-PCR in three independent HTM lines after 4 days at 40% oxygen compared to parallel cultures incubated at 5% oxygen. In these conditions miR-29b decreased significantly between 2- and 2.5-fold in two of the three cell lines analyzed and showed no significant change in a third line (Figure 4).

Role of miR-29b on changes in expression of extracellular matrix genes induced by chronic oxidative stress.: To investigate whether the downregulation of miR-29b observed in two cell lines could mediate alterations in gene expression

induced by chronic oxidative stress, the effects of incubation at 40% oxygen on the expression of six genes known to be regulated by miR-29b (*COL1A2, COL5A1, COL3A1, COL1A1, LAMC,* and *SPARC*) were analyzed in the same three HTM cell lines used in the previous experiment. The experiments were conducted in cells transfected with either control mimic or miR-29b mimic. Although there was a high level of variability in the effects of chronic oxidative stress on the expression of the selected genes, the two cell lines where miR-29b had been found to be downregulated more than twofold under oxidative stress conditions showed a significant increase in the expression of several genes regulated by miR-29b. In contrast, incubation at 40% oxygen had little effect on the expression of these genes in the cell line where miR-29b had not been found to be altered by chronic oxidative stress. In all cell lines, transfection with miR-29b mimic led to either a significant downregulation or decrease in the upregulation mediated by chronic oxidative stress of all genes analyzed compared to cultures transfected with control mimic (Figure 5).
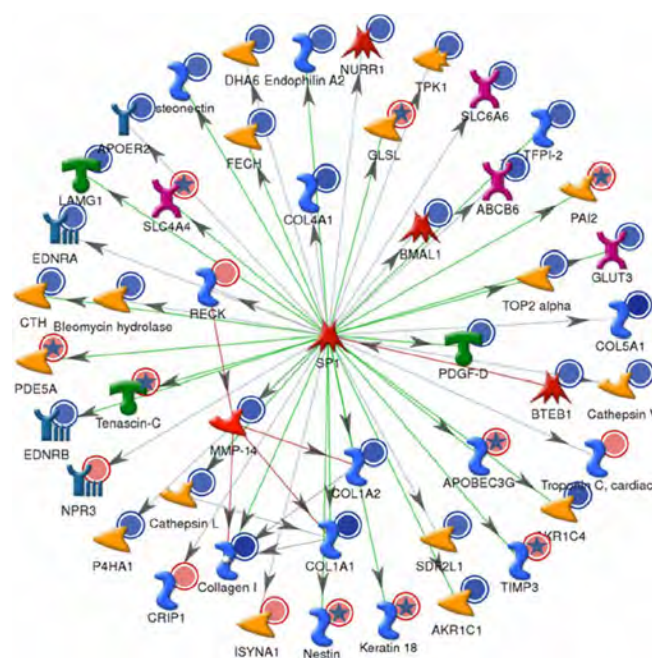

Figure 2. Genes known to be regulated by SP1 that showed significant differences in expression after transfection with miR-29b mimic by array analysis. Metacore analysis of the genes showing significant differences (p<0.5) in expression in the Affymetrix U133A2 arrays identified SP1 as the transcription factor more significantly (p= 4.82 E-106) associated with these gene expression changes. Green lines represent upregulation by SP1, red lines a downregulation, and gray lines an unspecified effect. Genes significantly upregulated in gene array analysis of cells transfected with miR-29b are labeled with red dots. Genes significantly downregulated by miR-29b are labeled with blue dots. Inconsistencies between the array data and the effects predicted by Metacore based on the literature are labeled with a star.

Effects of miR-29b on cytotoxicity: HTM cells transfected with control mimic or miR-29b mimic were subjected to 40% or 5% oxygen and analyzed for cytotoxicity after 5 days. Cells transfected with miR-29b mimic showed a significant decrease in cytotoxicity compared to the control in both oxygen concentrations (5 and 40%) except for HTM cell line 3 at 40% O_2, which showed a nonsignificant decrease in cytotoxicity (Figure 6).
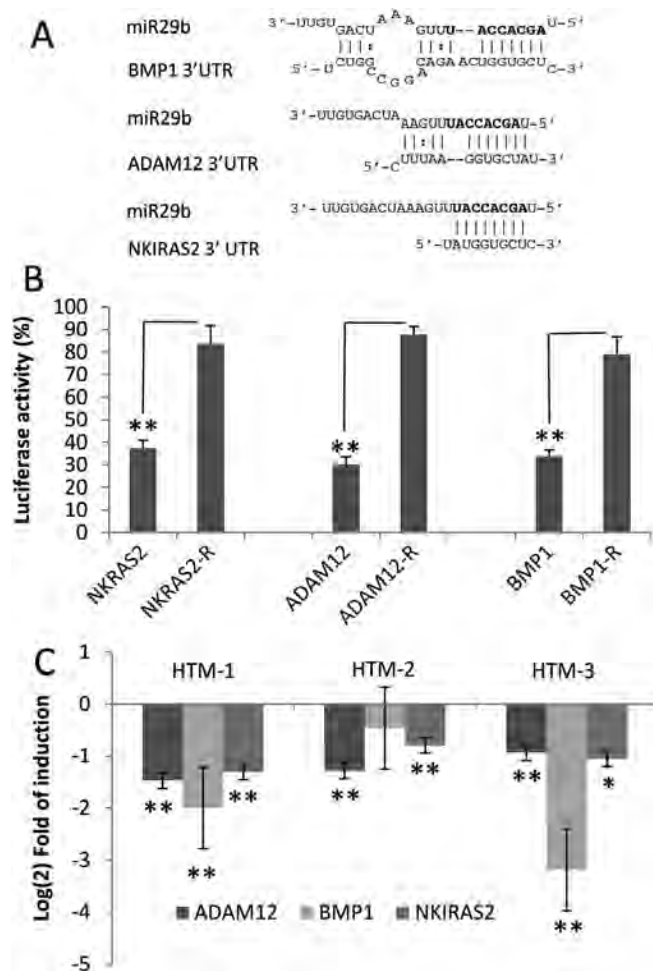

Figure 3. Targeting of the 3'-unstranslated regions of *BMP1*, *ADAM12*, and *NKIRAS2* by miR-29b. **A**: Predicted interactions between miR-29b with the 3'-unstranslated region (3' UTR) of *BMP1* (PicTar-Vert), *ADAM12* (TargetScan), and *NKRAS2* (PicTar-Vert). Seed regions are highlighted in bold. **B**: Luciferase activity in 293 cells cotransfected with psicheck vectors containing the 3'UTR or complementary sequence (R) from *BMP1*, *ADAM12*, or *NKIRAS2* and miR-29b or scramble. **C**: Changes in expression of *ADAM12*, *BMP1*, and *NKIRAS2* were measured by Q-PCR after transfection with miR-29b mimic or scramble. The figures represent the logarithm of the fold change in gene expression compared to cells transfected with scramble in three different cells lines. Bars represent standard error from three different experiments; one asterisk indicates a p≤0.05, and two asterisks indicate a p≤0.01.

DISCUSSION

Our results showed that miR-29b negatively regulates the expression in HTM cells of multiple genes involved in ECM synthesis, deposition, and remodeling. In addition, incubation under chronic oxidative stress conditions (4 days, 40% oxygen) resulted in a significant downregulation of miR-29b in two of the three HTM cell lines analyzed. This downregulation was associated with an increase in the expression of several ECM genes known to be regulated by miR-29b. The upregulation of these genes by chronic oxidative stress was inhibited by transfection with miR-29b mimic.

The multiple effects on the expression of ECM components observed in HTM cells were consistent with the antifibrotic activity previously reported for miR-29b in the
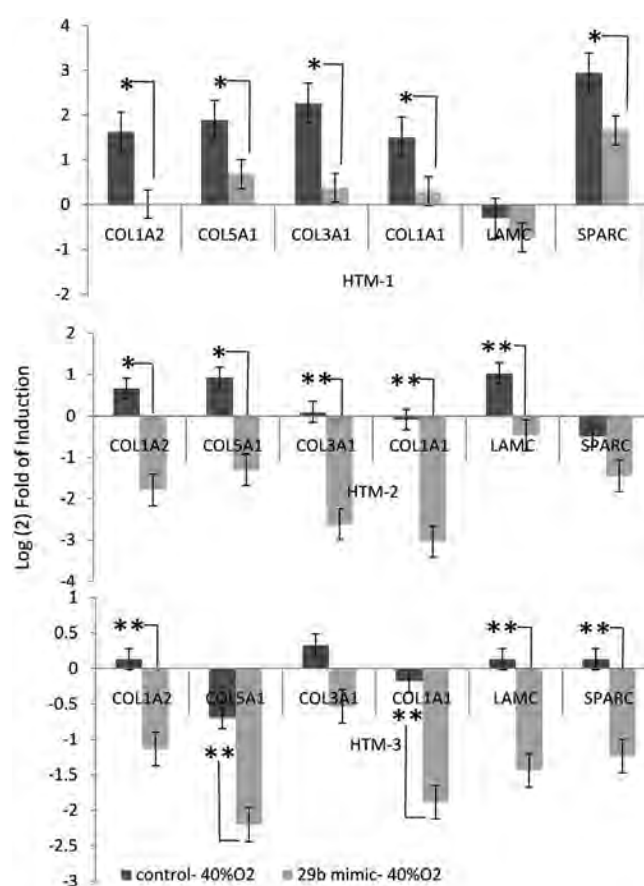

Figure 4. Changes in miR-29b induced by chronic oxidative stress. To investigate if miR-29b changes with chronic oxidative stress, three human trabecular meshwork (HTM) cell lines were incubated during 4 days at 40% oxygen, and the changes in the expression of miR-29b were quantified by quantitative–PCR (Q-PCR) and compared to nonstressed controls incubated at 5% oxygen. The figures represent the logarithm of the fold change in gene expression between cells incubated at 40% oxygen compared to controls. Bars represent standard error from three different measurements. One asterisk means p≤0.05.

heart [19]. These effects include the downregulation of validated targets, such as *COL1A1,COL1A2,COL3A1,FBN1*, and *SPARC* [19,22].

MiR-29b also downregulated numerous genes that have not been confirmed as direct targets of this miRNA. Some of these genes contained sequences in their 3'UTRs that are predicted to anneal to miR-29b and may potentially interact with miR-29b. Among these genes, *BMP1*, *ADAM12*, and *NKIRAS2* were confirmed by luciferase analysis to contain 3'UTRs that can be directly targeted by miR-29b and should be considered targets of this miRNA. However, many of the gene expression changes induced by miR-29b affected genes that lack any predicted targeting sequence for miR-29b and appear to be secondary targets. Pathway analysis indicated that a number of these genes are positively regulated by the transcription factor SP1, which is a validated target of miR-29b [23], suggesting that inhibition of SP1 by miR-29 may be an important factor in the overall effects on gene expression mediated by miR-29b.

Exposure to chronic oxidative stress conditions for 4 days resulted in a significant decrease in expression of miR-29b in two (HTM1 and HTM2) of the three cell lines analyzed. Interestingly, while these two cell lines showed increased

expression of several genes known to be validated targets of miR-29b, the only cell line where miR-29b was not downregulated (HTM3) showed no significant increase in the expression of these genes. The upregulation of ECM genes mediated by chronic oxidative stress in cells lines HTM1 and HTM2 was inhibited by transfection with miR-29b. These results suggest that downregulation of miR-29b could be a mechanism that mediates some of the alterations in ECM induced by chronic oxidative stress. The variability observed in the levels of upregulation of each gene analyzed between
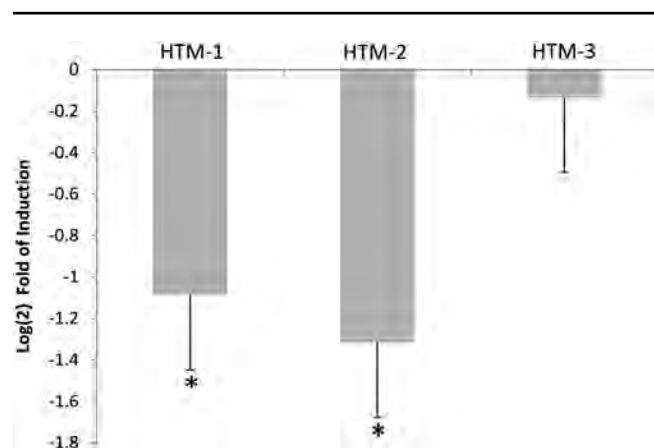

Figure 5. The role of miR-29b on changes in expression of extracellular matrix genes induced by chronic oxidative stress. To investigate whether miR-29b under chronic oxidative stress conditions could affect the changes in expression of several extracellular matrix (ECM) genes, three human trabecular meshwork (HTM) cell lines were transfected with miR-29b mimic or control mimic and incubated under oxidative stress conditions (40% O$_2$) for 4 days. The changes in expression of *COL1A2, COL5A1, COL3A1, COL1A1, LAMC1*, and *SPARC* compared to nonstressed controls incubated at 5% oxygen and transfected with control mimic were quantified by quantitative-PCR (Q- PCR). The figures represent the logarithm of the fold change in gene expression between cells incubated at 40% oxygen transfected with either miR-29b mimic or mimic control compared to control cultures (5% oxygen, mimic control) for three individual cell lines. Bars represent standard error from three different experiments. One asterisk means p≤0.05, and two asterisks mean p≤0.01.
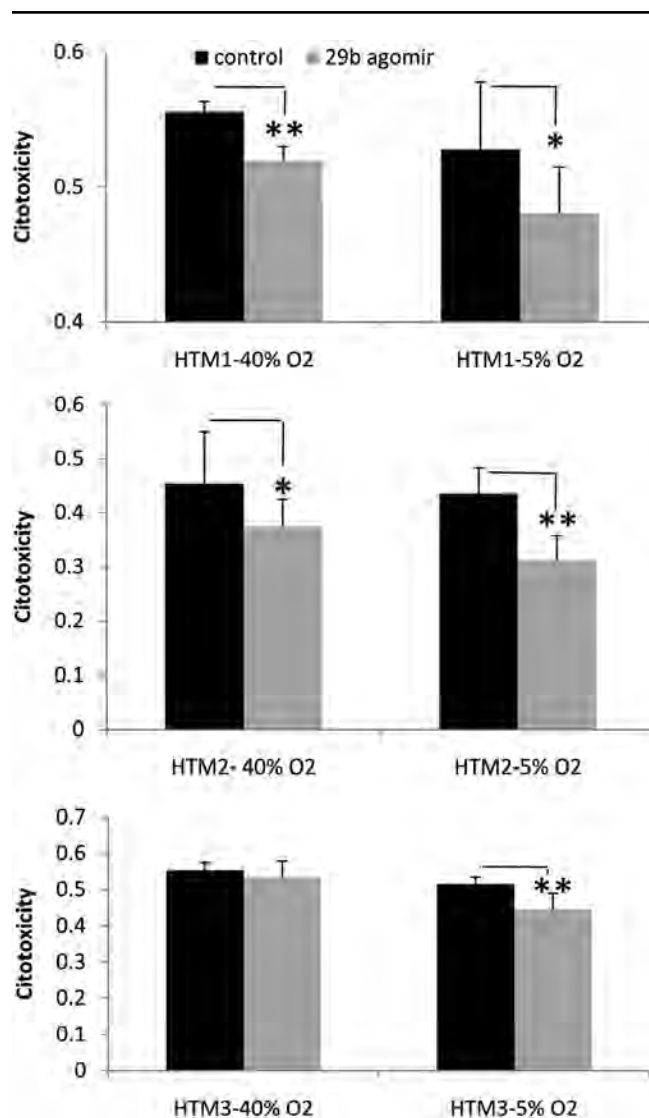

Figure 6. Effects of miR-29b on the cytotoxicity of human trabecular meshwork (HTM) cells. HTM cells transfected with miR-29b mimic showed significantly lower levels of cytotoxicity measured by lactate dehydrogenase release compared to cells transfected with control mimic when incubated at both 40% oxygen and 5% oxygen conditions. Bars represent standard error from three different experiments. One asterisk means p≤0.05, and two asterisks mean p≤0.01.

the two cell lines where miR-29b was significantly downregulated is likely to result from the influence of multiple pathways involved in the regulation of the ECM under oxidative stress conditions. However, our results suggest that miR-29b may be an important regulatory component of this process.

The genes selected for this study included important components of the ECM, such as *COL1A2*, *COL5A1*, *COL3A1*, *COL1A1*, *LAMC*, and the matricellular protein *SPARC* that is known to promote ECM deposition [24,25]. Increased expression of these genes could potentially influence the physiology of the outflow pathway by contributing to increased deposition of collagen and other ECM components in the TM [26-30]. Therefore, the variability observed in the effects of chronic oxidative stress on the expression of miR-29b could be relevant to understanding individual differences in susceptibility to pathophysiological alterations induced by chronic oxidative stress in the outflow pathway.

In addition to changes in the expression of ECM components, our results also showed that miR-29b had a protective effect and decreased cell death. Such effect on cell viability contrasts with the pro-apoptotic effects reported for this miRNA in other cell types [16,31,32]. Members of the miR-29 family, including miR-29b, have been demonstrated to activate *p53* by targeting *p85α* and *CDC42* [31]. Because of the known pro-apoptotic effects of *p53*, this function of miR-29b would initially be expected to increase apoptosis under chronic oxidative stress conditions. However, under mild stress conditions, p53 is also known to exert antioxidant and survival effects that are believed to be aimed at preventing oxidative damage and ensuring the survival and repair of cells encountering only low levels of damage [33]. Under the chronic oxidative conditions used in our model, cells might suffer only a moderated level of damage, which would lead to a pro-survival function of *p53*. Furthermore, transient expression of miR-29a, which shares the same seed region of miR-29b and also regulates p53 through targeting of p85α and *CDC42*, did not result in increased apoptosis in osteoblasts [31]. Thus, the pro-apoptotic effects reported for miR-29 may be dependent on the cell type or the specific stress conditions affecting the cells. It is also possible that additional targets of miR-29b that have not been characterized may be involved in the effects of miR-29b on cell survival in HTM cells. For instance, one of the new targets identified in this study, *NKRAS2*, is a negative modulator of *NFKB*, and its downregulation by miR-29b could potentially facilitate the anti-apoptotic effects of *NFKB*.

In conclusion, miR-29b negatively modulated the expression of collagens and other key components of the ECM in TM cells and decreased cytotoxicity in the presence of chronic oxidative stress. The downregulation of miR-29b observed in two cell lines could contribute to some of the alterations in ECM metabolism and cell viability mediated by chronic oxidative stress in HTM cells. The balance between the activation of ECM production induced by oxidative stress and the protective effects of miR-29b could be a relevant factor in understanding how oxidative damage may lead to increased deposition of ECM and decreased cellularity in the outflow pathway and contribute to the elevation of intra-ocular pressure in glaucoma. Strategies to increase miR-29 expression in TM cells may be beneficial to limit ECM deposition, prevent cell loss, and maintain normal levels of aqueous humor outflow facility.

REFERENCES
1. Izzotti A, Bagnis A, Sacca SC. The role of oxidative stress in glaucoma. Mutat Res 2006; 612:105-14. [PMID: 16413223]
2. Izzotti A, Sacca SC, Cartiglia C, De Flora S. Oxidative deoxyribonucleic acid damage in the eyes of glaucoma patients. Am J Med 2003; 114:638-46. [PMID: 12798451]
3. Babizhayev MA, Bunin A. Lipid peroxidation in open-angle glaucoma. Acta Ophthalmol (Copenh) 1989; 67:371-7. [PMID: 2801038]
4. Zanon-Moreno V, Marco-Ventura P, Lleo-Perez A, Pons-Vazquez S, Garcia-Medina JJ, Vinuesa-Silva I, Moreno-Nadal MA, Pinazo-Duran MD. Oxidative stress in primary open-angle glaucoma. J Glaucoma 2008; 17:263-8. [PMID: 18552610]
5. Sacca SC, Izzotti A, Rossi P, Traverso C. Glaucomatous outflow pathway and oxidative stress. Exp Eye Res 2007; 84:389-99. [PMID: 17196589]
6. Sacca SC, Pascotto A, Camicione P, Capris P, Izzotti A. Oxidative DNA damage in the human trabecular meshwork: clinical correlation in patients with primary open-angle glaucoma. Arch Ophthalmol 2005; 123:458-63. [PMID: 15824217]
7. Ohia SE, Opere CA, Leday AM. Pharmacological consequences of oxidative stress in ocular tissues. Mutat Res 2005; 579:22-36. [PMID: 16055157]
8. Alvarado J, Murphy C, Juster R. Trabecular meshwork cellularity in primary open-angle glaucoma and nonglaucomatous normals. Ophthalmology 1984; 91:564-79. [PMID: 6462622]
9. Fatma N, Kubo E, Toris CB, Stamer WD, Camras CB, Singh DP. PRDX6 attenuates oxidative stress- and TGFbeta-induced abnormalities of human trabecular meshwork cells. Free Radic Res 2009; 43:783-95. [PMID: 19572226]
10. Ueda J, Wentz-Hunter K, Yue BY. Distribution of myocilin and extracellular matrix components in the juxtacanalicular tissue of human eyes. Invest Ophthalmol Vis Sci 2002; 43:1068-76. [PMID: 11923248]
11. Wu L, Fan J, Belasco JG. MicroRNAs direct rapid deadenylation of mRNA. Proc Natl Acad Sci USA 2006; 103:4034-9. [PMID: 16495412]
12. Filipowicz W, Bhattacharyya SN, Sonenberg N. Mechanisms of post-transcriptional regulation by microRNAs: are the

answers in sight? Nat Rev Genet 2008; 9:102-14. [PMID: 18197166]

13. Stefani G, Slack FJ. Small non-coding RNAs in animal development. Nat Rev Mol Cell Biol 2008; 9:219-30. [PMID: 18270516]

14. Li Z, Hassan MQ, Jafferji M, Aqeilan RI, Garzon R, Croce CM, van Wijnen AJ, Stein JL, Stein GS, Lian JB. Biological functions of miR-29b contribute to positive regulation of osteoblast differentiation. J Biol Chem 2009; 284:15676-84. [PMID: 19342382]

15. Fabbri M, Garzon R, Cimmino A, Liu Z, Zanesi N, Callegari E, Liu S, Alder H, Costinean S, Fernandez-Cymering C, Volinia S, Guler G, Morrison CD, Chan KK, Marcucci G, Calin GA, Huebner K, Croce CM. MicroRNA-29 family reverts aberrant methylation in lung cancer by targeting DNA methyltransferases 3A and 3B. Proc Natl Acad Sci USA 2007; 104:15805-10. [PMID: 17890317]

16. Mott JL, Kobayashi S, Bronk SF, Gores GJ. mir-29 regulates Mcl-1 protein expression and apoptosis. Oncogene 2007; 26:6133-40. [PMID: 17404574]

17. Pekarsky Y, Santanam U, Cimmino A, Palamarchuk A, Efanov A, Maximov V, Volinia S, Alder H, Liu CG, Rassenti L, Colin GA, Hagan JP, Kipps T, Croce CM. Tcl1 expression in chronic lymphocytic leukemia is regulated by miR-29 and miR-181. Cancer Res 2006; 66:11590-3. [PMID: 17178851]

18. Sengupta S, den Boon JA, Chen IH, Newton MA, Stanhope SA, Cheng YJ, Chen CJ, Hildesheim A, Sugden B, Ahlquist P. MicroRNA 29c is down-regulated in nasopharyngeal carcinomas, up-regulating mRNAs encoding extracellular matrix proteins. Proc Natl Acad Sci USA 2008; 105:5874-8. [PMID: 18390668]

19. van Rooij E, Sutherland LB, Thatcher JE, DiMaio JM, Naseem RH, Marshall WS, Hill JA, Olson EN. Dysregulation of microRNAs after myocardial infarction reveals a role of miR-29 in cardiac fibrosis. Proc Natl Acad Sci USA 2008; 105:13027-32. [PMID: 18723672]

20. Stamer WD, Seftor RE, Williams SK, Samaha HA, Snyder RW. Isolation and culture of human trabecular meshwork cells by extracellular matrix digestion. Curr Eye Res 1995; 14:611-7. [PMID: 7587308]

21. Helbig H, Hinz JP, Kellner U, Foerster MH. Oxygen in the anterior chamber of the human eye. Ger J Ophthalmol 1993; 2:161-4. [PMID: 8334391]

22. Kapinas K, Kessler CB, Delany AM. miR-29 suppression of osteonectin in osteoblasts: Regulation during differentiation and by canonical Wnt signaling. J Cell Biochem 2009; 108:216-24. [PMID: 19565563]

23. Garzon R, Liu S, Fabbri M, Liu Z, Heaphy CE, Callegari E, Schwind S, Pang J, Yu J, Muthusamy N, Havelange V, Volinia S, Blum W, Rush LJ, Perrotti D, Andreeff M, Bloomfield CD, Byrd JC, Chan K, Wu LC, Croce CM, Marcucci G. MicroRNA-29b induces global DNA hypomethylation and tumor suppressor gene reexpression in acute myeloid leukemia by targeting directly DNMT3A and 3B and indirectly DNMT1. Blood 2009; 113:6411-8. [PMID: 19211935]

24. Bradshaw AD, Reed MJ, Sage EH. SPARC-null mice exhibit accelerated cutaneous wound closure. J Histochem Cytochem 2002; 50:1-10. [PMID: 11748289]

25. Bradshaw AD, Puolakkainen P, Dasgupta J, Davidson JM, Wight TN, Helene Sage E. SPARC-null mice display abnormalities in the dermis characterized by decreased collagen fibril diameter and reduced tensile strength. J Invest Dermatol 2003; 120:949-55. [PMID: 12787119]

26. Rhee DJ, Fariss RN, Brekken R, Sage EH, Russell P. The matricellular protein SPARC is expressed in human trabecular meshwork. Exp Eye Res 2003; 77:601-7. [PMID: 14550402]

27. Norose K, Clark JI, Syed NA, Basu A, Heber-Katz E, Sage EH, Howe CC. SPARC deficiency leads to early-onset cataractogenesis. Invest Ophthalmol Vis Sci 1998; 39:2674-80. [PMID: 9856777]

28. Bassuk JA, Birkebak T, Rothmier JD, Clark JM, Bradshaw A, Muchowski PJ, Howe CC, Clark JI, Sage EH. Disruption of the Sparc locus in mice alters the differentiation of lenticular epithelial cells and leads to cataract formation. Exp Eye Res 1999; 68:321-31. [PMID: 10079140]

29. Zhou XD, Xiong MM, Tan FK, Guo XJ, Arnett FC. SPARC, an upstream regulator of connective tissue growth factor in response to transforming growth factor beta stimulation. Arthritis Rheum 2006; 54:3885-9. [PMID: 17133596]

30. Rhee DJ, Haddadin RI, Kang MH, Oh DJ. Matricellular proteins in the trabecular meshwork. Exp Eye Res 2009; 88:694-703. [PMID: 19101543]

31. Park SY, Lee JH, Ha M, Nam JW, Kim VN. miR-29 miRNAs activate p53 by targeting p85 alpha and CDC42. Nat Struct Mol Biol 2009; 16:23-9. [PMID: 19079265]

32. Wang Y, Lee CG. MicroRNA and cancer--focus on apoptosis. J Cell Mol Med 2009; 13:12-23. [PMID: 19175697]

33. Sablina AA, Budanov AV, Ilyinskaya GV, Agapova LS, Kravchenko JE, Chumakov PM. The antioxidant function of the p53 tumor suppressor. Nat Med 2005; 11:1306-13. [PMID: 16286925]